Acta Crystallographica Section B
Structural Science
ISSN 0108-7681

New phosphate langbeinites, $K_2MTi(PO_4)_3$ (M = Er, Yb or Y), and an alternative description of the langbeinite framework

Stefan T. Norberg

Inorganic Chemistry, Chalmers University of Technology, SE-412 96 Göteborg, Sweden

Correspondence e-mail: stn@inoc.chalmers.se

Received 7 May 2002
Accepted 31 July 2002

Three new potassium rare-earth/titanium phosphate structures, $K_2ErTi(PO_4)_3$ (KErTP), $K_2YbTi(PO_4)_3$ (KYbTP) and $K_2YTi(PO_4)_3$ (KYTP), are presented, all of which are characterized by single-crystal X-ray diffraction studies. In addition, a fourth structure, $K_2CrTi(PO_4)_3$ (KCrTP), has been reinvestigated. All structures are isostructural to the langbeinite-type structure and result from changes made to the growth constituents in high-temperature flux-growth experiments intended to give structurally modified potassium titanyl phosphate (KTP). The two crystallographically independent octahedra sites (site symmetry 3) have a mixed Ti/M (M = Er, Yb, Y or Cr) population, although the rare-earth metals favour one site while chromium favours the other. An alternative approach for the description of the channels and cation cages in langbeinite and related structures is given using $[M_5X_6O_{39}]$ units. The framework of langbeinite is compared with that of nasicon using these alternative building units. All of the investigated structures crystallize in space group $P2_13$ with $Z = 4$; $a = 10.1053$ (2) Å, $R = 0.023$ (KErTP); $a = 10.0939$ (8) Å, $R = 0.022$ (KYbTP); $a = 10.1318$ (6) Å, $R = 0.047$ (KYTP); $a = 9.8001$ (2) Å, $R = 0.016$ (KCrTP).

1. Introduction

The new phosphate langbeinite structures belong to a large group of synthetic minerals. The name langbeinite originates from the naturally occurring mineral langbeinite $[K_2Mg_2(SO_4)_3]$, which was structurally characterized by Zemann & Zemann (1957). These compounds have the general chemical formula $A_xB_2(XO_4)_3$, and crystallize in a high-temperature cubic phase, *i.e.* space group $P2_13$. Several different mechanisms have been suggested (Lissalde *et al.*, 1979; Yamada *et al.*, 1981; Percival *et al.*, 1989; Moriyoshi *et al.*, 1996) in order to describe the phase transitions that occur in the langbeinite family. However, the structure of the low-temperature phase has only been characterized for a few langbeinite compounds. The complexity is well illustrated by the low-temperature phase transitions of $Tl_2Cd_2(SO_4)_3$ (Brezina & Glogarova, 1972; Guelylah *et al.*, 2000):

$$P2_13 \xrightarrow{128K} P2_1 \xrightarrow{119K} P1 \xrightarrow{98K} P2_12_12_1.$$

The sulfate langbeinites $[A_2^{I}B_2^{II}(SO_4)_3]$ are the most frequently investigated and best known group of langbeinites, and they have attracted a great deal of interest due to their ferroelectric/ferroelastic behaviour. These properties have been studied in some sulfate langbeinites, *e.g.* $(NH_4)_2Cd_2(SO_4)_3$ (Jona & Pepinsky, 1956), $Tl_2Cd_2(SO_4)_3$ (Brezina & Glogarova, 1972), $Rb_2Cd_2(SO_4)_3$ (Hikita *et al.*,

1976) and $K_2Cd_2(SO_4)_3$ (Abrahams & Bernstein, 1977; Lissalde *et al.*, 1979). The different sulfate compounds are built from combinations of large monovalent cations (A^{I} = NH_4, K, Rb, Cs or Tl) and smaller divalent cations (B^{II} = Mg, Ca, Mn, Fe, Co, Ni, Zn or Cd). Langbeinites with other oxyanions are also known to exist, of which $KTi_2(PO_4)_3$ (Masse *et al.*, 1972), $(NH_4)_2Mn_2(SeO_4)_3$ (Kohler & Franke, 1964), $Cs_2Mn_2(CrO_4)_3$ (Cord *et al.*, 1971) and $Rb_2Co_2(MoO_4)_3$ (Klevtsov *et al.*, 1988) are some examples.

Phosphate langbeinites form a small group of compounds where most of those that are structurally characterized contain titanium. The structure of $Na_2MTi(PO_4)_3$ (M = Fe, Cr) has been determined by Isasi & Daidouh (2000) from powder-diffraction data, while the structures of $KTi_2(PO_4)_3$, $K_2Ti_2(PO_4)_3$ and $K_{1+x}Ti_{2-y}Al_y(PO_4)_3$ (Masse *et al.*, 1972; Leclaire *et al.*, 1989; Slobodyanik *et al.*, 1991) have been determined from single-crystal data. Powder-diffraction studies indicate that $K_2CrTi(PO_4)_3$, $A_2MTi(PO_4)_3$ (A = K, Rb, Tl; M = Cr, Fe) and $K_2TiV(PO_4)_3$ have a langbeinite-type structure (Boudjada & Perret, 1977; Perret & Boudjada, 1979; Rangan & Gopalakrishnan, 1994). These monophosphates can be summarized as having the general chemical formula $A_xM_2(PO_4)_3$.

Phosphate langbeinites are scarce because most $A_xM_2(PO_4)_3$ compounds crystallize in the related nasicon-type structure [$Na_3Zr_2(PO_4)(SiO_4)_2$; Sljukic *et al.*, 1967; Von Alpen *et al.*, 1979]. $NaTi_2(PO_4)_3$ (Ivanov *et al.*, 1980), $RbTi_2(PO_4)_3$ (Hazen *et al.*, 1994) and $Na_3Cr_2(PO_4)_3$ (Genkina *et al.*, 1991) are such examples. The crystallization product is to some degree dependent on the number (x) of A cations required by the $M_2(PO_4)_3$ framework and the ionic radius of the A cation (Perret, 1988; Rangan & Gopalakrishnan, 1994). Some $A_xM_2(PO_4)_3$ compounds can crystallize in either form; one example is $KTi_2(PO_4)_3$, structurally determined as cubic langbeinite by Masse *et al.* (1972) and as rhombohedral nasicon by Lunezheva *et al.* (1989). Both langbeinite and nasicon consist of a three-dimensional framework built of MO_6 octahedra connected by PO_4 tetrahedra. The monovalent or divalent cations (A = Na^+, K^+, Rb^+, Sr^{2+} or Ba^{2+}) occupy channels and cavities formed by the framework. The langbeinite framework creates closed cavities that trap the cations while the nasicon-type structure has channels that result in a high ion mobility.

The bonding characteristics of KErTP, KYbTP, KYTP and KCrTP are structurally investigated. A new model for describing the cavities and channels in langbeinite and langbeinite-related structures is presented. Building units of $[M_5X_6O_{39}]$ are used as a complement to the smaller $[M_2X_3O_{18}]$ building blocks. The structures of langbeinite and nasicon are compared with each other using the new building unit.

2. Experimental

2.1. Preparation of crystals

The KErTP, KYbTP and KYTP crystals originate from crystal-growth experiments intended to produce rare-earth modified KTP (potassium titanyl phosphate, $KTiOPO_4$; Tordjman *et al.*, 1974). Earlier experiments have shown that small amounts of chromium can co-host with titanium inside the distorted TiO_6 octahedra (Bolt, 1993; Norberg *et al.*, 2000). The effects due to the addition of a rare-earth oxide or rare-earth chloride in KTP crystal-growth fluxes were therefore explored. The high-temperature solution growth experiments were carried out in 35 ml platinum crucibles using the $K_6P_4O_{13}$ self-flux method (Jacco *et al.*, 1984). Equimolar amounts of $K_6P_4O_{13}$ flux and KTP growth constituents were used since this has been proven to result in large KTP crystals. This gave us a starting mixture containing TiO_2, KH_2PO_4 and K_2HPO_4 with a molar ratio of 1:3:2. Rare-earth oxides (Y and Yb) and rare-earth chlorides (Pr, Nd, Sm and Er) were later added to the mixture.

KYTP was crystallized from 9.5 g of the start mixture and 0.5 g of Y_2O_3, resulting in a Ti^{4+}/Y^{3+} ratio of 2.6:1. KYbTP was crystallized in the same way from 9.5 g of the start mixture and 1.0 g of Yb_2O_3, resulting in a Ti^{4+}/Yb^{3+} ratio of 2.3:1. The KErTP crystallization was obtained from a 10 g mixture of TiO_2, KH_2PO_4, K_2HPO_4 and $ErCl_3{\cdot}6H_2O$ in a molar ratio of 1:3:2:0.3, giving a Ti^{4+}/Er^{3+} ratio of 3.3:1. All batches were carefully mixed and thereafter slowly heated to 1273 K over a four-day period, in order to obtain a homogeneous melt. The melts were kept at 1273 K for 60 h and finally cooled to 1023 K at 1.4 K h^{-1}. Experimental details for KCrTP can be found in Norberg *et al.* (2000).

All crystals were easily recovered by dissolving the flux in hot water. The KYTP batch produced 0.9 g of crystalline material, with a large number of tetrahedrally shaped crystals of about 2 mm in size. The KYbTP batch gave 1.5 g of crystalline material including some large crystals (1–2 mm) of irregular shape and a large number of small crystals with perfect tetrahedral shape. The KErTP batch gave 1.0 g of crystalline material with a pinkish colour that was due to crystallized $ErPO_4$. A small number of the crystals had a tetrahedral shape, indicating that they were of the langbeinite-type structure. All crystals in the KYTP, KYbTP and KErTP batch were colourless and free from flux residues. It should also be noted that the addition of $MCl_3{\cdot}xH_2O$ (M = Pr, Nd and Sm) to a KTP growth flux produced rare-earth phosphates but no langbeinite crystals.

Energy-dispersive X-ray (EDX) analysis (electro-scan S4–8DV equipped with a Link eX1 EDX system) was used to verify the atomic content of the structurally determined crystals. Crystals from the X-ray diffraction experiment and random crystals from the growth batches were analysed. All measurements indicated a Ti/M (M = Er, Yb, Y or Cr) ratio close to 1:1 and a K/P ratio of 2:3, as was expected for $K_{1+x}M_xTi_{2-x}(PO_4)_3$ crystals with x = 1.

2.2. Data collection and structure refinement

All data were collected with an Enraf–Nonius CAD-4 diffractometer using Mo $K\alpha$ radiation. An analytical absorption correction (Alcock, 1974) was applied to the collected data and smaller variations in intensity were corrected using

Table 1
Experimental details.

	KErTP	KYbTP	KYTP	KCrTP
Crystal data				
Chemical formula	$K_2ErTiP_3O_{12}$	$K_2YbTiP_3O_{12}$	$K_2YTiP_3O_{12}$	$K_2CrTiP_3O_{12}$
Chemical formula weight	578.25	584.03	499.89	462.98
Cell setting, space group	Cubic, $P2_13$	Cubic, $P2_13$	Cubic, $P2_13$	Cubic, $P2_13$
a (Å)	10.1053 (2)	10.0939 (8)	10.1318 (6)	9.8001 (2)
V (Å^3)	1031.92 (4)	1028.4 (2)	1040.06 (11)	941.22 (4)
Z	4	4	4	4
D_x (Mg m^{-3})	3.722	3.772	3.192	3.267
Radiation type	Mo $K\alpha$	Mo $K\alpha$	Mo $K\alpha$	Mo $K\alpha$
No. of reflections for cell parameters	20	24	18	23
θ range (°)	26.62–29.76	23.99–29.78	7.54–17.31	31.30–34.90
μ (mm^{-1})	10.187	11.155	7.646	3.468
Temperature (K)	293 (2)	293 (2)	293 (2)	293 (2)
Crystal form, colour	Tetrahedron, colourless	Tetrahedron, colourless	Tetrahedron, colourless	Tetrahedron, green
Crystal size (mm)	0.06 × 0.06 × 0.05	0.035 × 0.030 × 0.025	0.015 × 0.012 × 0.010	0.085 × 0.085 × 0.065
Data collection				
Diffractometer	Enraf–Nonius CAD-4 diffractometer	Enraf–Nonius CAD-4 diffractometer	Enraf–Nonius CAD-4 diffractometer	Enraf–Nonius CAD-4 diffractometer
Data collection method	ω–2θ scans	ω–2θ scans	ω–2θ scans	ω–2θ scans
Absorption correction	Analytical	Analytical	Analytical	Analytical
T_{min}	0.567	0.687	0.917	0.759
T_{max}	0.650	0.753	0.933	0.813
No. of measured, independent and observed parameters	3285, 1008, 967	6213, 1008, 904	3303, 1014, 701	4496, 1394, 1346
Criterion for observed reflections	$F^2 > 2\sigma(F^2)$	$F^2 > 2\sigma(F^2)$	$F^2 > 2\sigma(F^2)$	$F^2 > 2\sigma(F^2)$
R_{int}	0.048	0.063	0.107	0.027
θ_{max} (°)	29.91	29.94	29.9	34.98
Range of h, k, l	$-14 \rightarrow h \rightarrow 0$ $-14 \rightarrow k \rightarrow 0$ $-14 \rightarrow l \rightarrow 14$	$-14 \rightarrow h \rightarrow 0$ $-14 \rightarrow k \rightarrow 14$ $-14 \rightarrow l \rightarrow 14$	$-14 \rightarrow h \rightarrow 0$ $-14 \rightarrow k \rightarrow 0$ $-14 \rightarrow l \rightarrow 14$	$-15 \rightarrow h \rightarrow 0$ $-15 \rightarrow k \rightarrow 0$ $-15 \rightarrow l \rightarrow 15$
No. and frequency of standard reflections	3 every 120 min	3 every 120 min	3 every 120 min	3 every 120 min
Refinement				
Refinement on	F^2	F^2	F^2	F^2
$R[F^2>2\sigma(F^2)]$, $wR(F^2)$, S	0.023, 0.077, 1.06	0.022, 0.066, 1.081	0.047, 0.18, 1.188	0.016, 0.052, 1.047
No. of reflections and parameters used in refinement	1008, 61	1008, 60	1014, 60	1394, 61
H-atom treatment	None	None	None	None
Weighting scheme	$w = 1/[\sigma^2(F^2) + 0.008(F^2)^2]$	$w = 1/[\sigma^2(F^2) + 0.045(F^2)^2]$	$w = 1/[\sigma^2(F^2) + 0.025(F^2)^2]$	$w = 1/[\sigma^2(F^2) + 0.0035(F^2)^2]$
$(\Delta/\sigma)_{max}$	0.00018	0.000041	0.000038	0.00016
$\Delta\rho_{max}$, $\Delta\rho_{min}$ (e Å^{-3})	0.6, −0.76	1.28, −0.93	1.65, −2.22	0.42, −0.47
Extinction method	Isotropic Gaussian	None	None	Isotropic Gaussian
Extinction coefficient	90 (22) × 10^2	–	–	114 (19) × 10^2

Computer programs used: *CAD-4 Software* (Enraf–Nonius, 1989); *Xtal*3.71 (Hall *et al.*, 2000) programs *DIFDAT*, *SORTRF*, *ADDREF*, *ABSORB*, *CRYLSQ*, *BONDLA*, *ATABLE*, *CIFIO*, *LATCON*; *SHELXS*97 (Sheldrick, 1997).

standard reflections. Symmetry-equivalent reflections were averaged while keeping the Friedel mates separated. All intensities were subjected to a Fisher test (Hamilton, 1964); intensities consistent with the measurement statistics were retained and the others were adjusted according to the scattering of equivalents. The systematic absences of (h00; $h = 2n + 1$; h, k, l cyclic permutable) suggested space group $P2_13$. Further details concerning the data collection and refinement procedure can be found in Table 1.[1]

The structure of KErTP was determined by direct methods in the *SHELXS*97 program (Sheldrick, 1997). All further least-square refinements were performed using the *Xtal*3.71 software package (Hall *et al.*, 2000). The M—O bond distances of 2.026 (7)–2.109 (9) Å indicated a mixed population of Ti and Er at both crystallographically independent octahedron sites (the combined effective radius of Ti^{IV} and O is 2.01 Å; Shannon, 1976). It was not possible to separate Ti and Er in two atomic positions at the respective octahedron site. The atomic position and anisotropic displacement parameters of Ti and Er were therefore constrained to be identical at each atomic site, and the site occupancy was set at 1.00.

[1] Supplementary data for this paper are available from the IUCr electronic archives (Reference: OS0095). Services for accessing these data are described at the back of the journal.

The potassium population parameter was set to refine freely in the initial phase of the least-square refinement, since the general chemical formula of KErTP is $K_{1+x}Er_xTi_{2-x}(PO_4)_3$. The total cation population was restricted to 2.00 because of the structure of the langbeinite framework. The occupancy parameter at both cation sites ended up close to 1.00 and was therefore fixed at 1.00 in the final refinement. The total occupancies of Ti and Er were fixed at 1.00, as both the cation population parameter and the EDX measurement indicated a Ti/Er ratio of 1:1. An isotropic extinction parameter (Zachariasen, 1967) was refined using Larson's implementation (Larson, 1970). About 15% of the reflections were affected by extinction with a maximum correction of $y = 0.88$ for the 0 1 3 reflection (the observed structure factor is $F_{obs} = yF_{kin}$, where F_{kin} is the kinematic value of the structure factor). The refined Flack (1983) parameter of 0.04 (3) indicates that the crystals used for the data collection were of single domain.

KYbTP was refined in the same way as KErTP using the same initial coordinates. As the isotropic extinction parameter refined to zero, it was excluded in the final refinement. The refined Flack parameter of 0.00 (3) indicates that the crystal was of single domain.

The atomic positions in KYTP are inverted compared with those of KErTP, and the small crystal used in the data collection showed no extinction. The Flack parameter refined to −0.10 (5), and it is clear from both twin refinements, using domains of different polarity and separate refinement of the inverted structure, that the absolute configuration has been determined.

KCrTP was refined in the same way as KErTP, and the isotropic extinction parameter influenced 10% of the reflections with a maximum correction of $y = 0.87$ for the 0 3 1 reflection. The refined Flack parameter of 0.02 (2) indicates that the crystals used for the data collection were of a single domain.

The atomic fractional coordinates, occupation and displacement parameters for $K_2ErTi(PO_4)_3$, $K_2YbTi(PO_4)_3$ and $K_2YTi(PO_4)_3$ are listed in the supplementary material.

3. Structure description

3.1. The langbeinite framework

The three-dimensional framework in the langbeinite-type structure consists of MO_6 octahedra and XO_4 tetrahedra and allows for cations to be located in large structural cages. The complex cubic structure is built from isolated XO_4 tetrahedra, sharing each corner with a MO_6 octahedron. All MO_6 octahedra are separated from each other and no electron delocalization can occur between them. Furthermore, the structure's framework is described on the basis of small building blocks. These building blocks are composed of two MO_6 octahedra linked together by three XO_4 tetrahedra to give rod-shaped blocks of $[M_2X_3O_{18}]$. The stacking of these building blocks is not intuitive since it is a complex procedure. Fig. 1(*a*) illustrates how each of the three XO_4 tetrahedra in the building block connects to two other building blocks. The stacking of building blocks can also be described with rods as illustrated in Fig. 1(*b*). A bond between individual rods indicates that the connected MO_6 octahedra are close to each other and bridged together by two XO_4 tetrahedra.

All large cations (*e.g.* K^+, Rb^+ *etc.*) are trapped in cages formed by the three-dimensional framework. The two crystallographically independent cation sites are located in the same cation cage and are within bonding distance of 18 O atoms (nine each). These O atoms are part of seven MO_6 octahedra connected together by XO_4 tetrahedra, forming an enclosed cage as shown in Fig. 2. The cation separation in the cage is approximately 3.9 Å.

In the usual description of the langbeinite structure with $[M_2X_3O_{18}]$ blocks, there is a tendency to overlook the existence of two different kinds of bridging between neighbouring MO_6 octahedra. The shortest bridging distance is inherent in the $[M_2X_3O_{18}]$ building block and is formed by three XO_4 tetrahedra between two octahedra with planes facing each

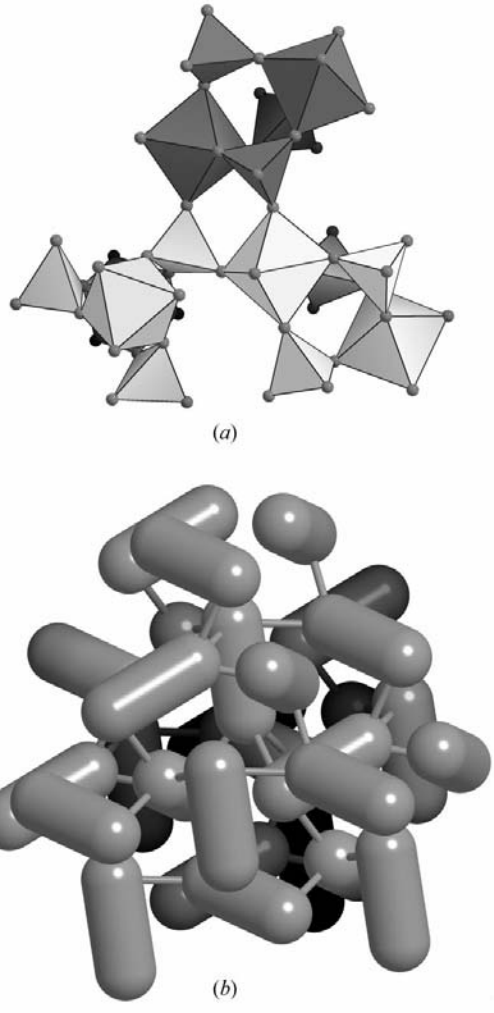

Figure 1
The $[M_2X_3O_{18}]$ building blocks are formed as seen in (*a*). Each building block is surrounded by 12 neighbouring building blocks, and the complex stacking pattern is shown in (*b*), where each thick rod represents an $[M_2X_3O_{18}]$ block.

other. A slightly longer bridging distance is the result of two bridging tetrahedra between octahedra with their edges opposite each other. The difference in bridging distance between these two is approximately 0.3 Å.

3.2. Visualization of cation cages and channels

As a complement to the commonly used building block $[M_2X_3O_{18}]$, an alternative building unit $[M_5X_6O_{39}]$ is proposed. The main purpose of this new unit is to visualize the cages and channels formed in langbeinite and related structures. This new building unit contains five MO_6 octahedra and six XO_4 tetrahedra (see Fig. 3). However, this new unit shares polyhedra with neighbouring units. The commonly used building block shares O atoms in the usual fashion, but not polyhedra. The new approach simplifies the comparison of langbeinite and nasicon, which have the same general formula (see Fig. 4). The nasicon structure allows for fast ion conductivity, and Fig. 4 shows the structure of langbeinite and nasicon using the alternative polyhedra instead of MO_6 octahedra and XO_4 tetrahedra. The zigzag pattern of the cations in the nasicon channels is clearly visible, and the channels themselves are easily observed. This approach to depicting cation cages *etc.* might be appropriate for other structures.

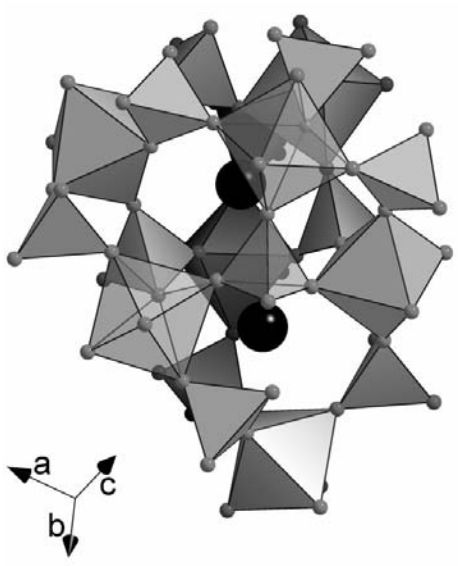

Figure 2
Polyhedra view of the cation cage with two enclosed cations. The foremost layer of polyhedra is slightly transparent in order to enhance the view of the cation cage.

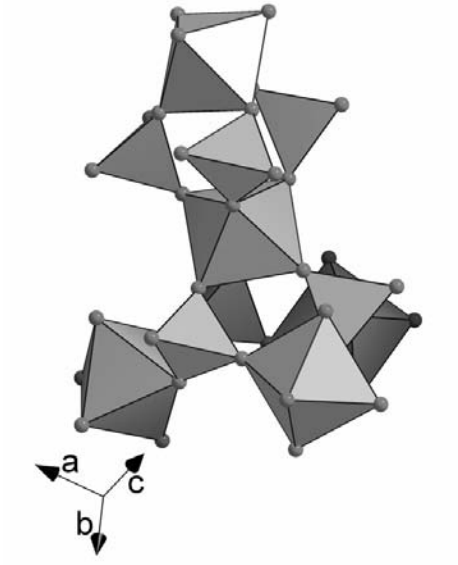

Figure 3
Polyhedra view of the complementary $[M_5X_6O_{39}]$ building unit.

4. Result and discussion

The structures of KErTP, KYbTP, KYTP and KCrTP are isostructural and belong to the langbeinite-type structure described in the previous section. The three rare-earth/titanium-based langbeinite structures, *i.e.* $K_2MTi(PO_4)_3$ (M = Er, Yb, Y), are similar when it comes to bond distances, volume and distortion of the M/TiO_6 octahedra and PO_4 tetrahedra, thermal-displacement parameters *etc.*, but in some respects KCrTP differs substantially from the others. All significant bond distances in the structurally characterized phosphate langbeinites are given in Table 2.

The MO_6 octahedra in the structures of KErTP, KYbTP, KYTP and KCrTP are regular, with only minor variations in the bond distances. M (M = Ti, Er, Yb, Y or Cr) is situated in the centre of the respective octahedron. There is, however, a small difference in volume between the crystallographically

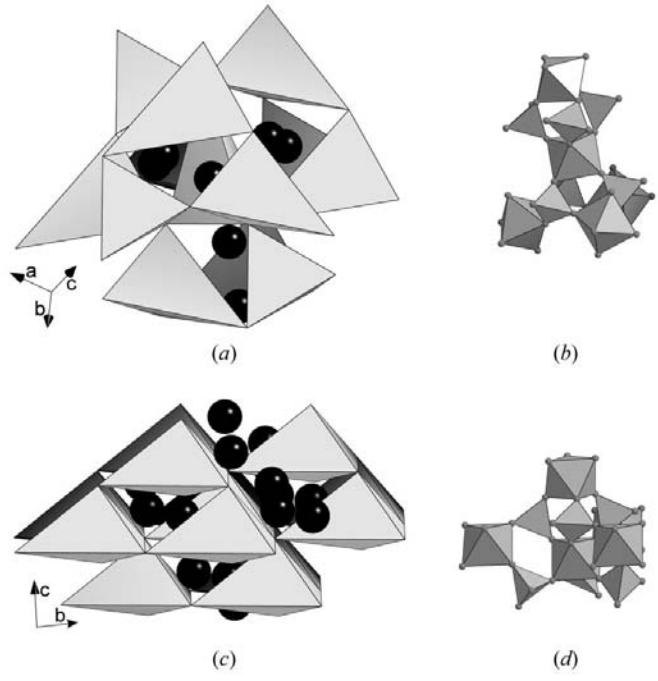

Figure 4
(*a*) and (*c*) depict the langbeinite- and nasicon-type structures using $[M_5X_6O_{39}]$ building units [see (*b*) and (*d*)].

Table 2
Bond lengths (Å) in the KErTP, KYbTP, KYTP and KCrTP structures.

	KErTP	KYbTP	KYTP	KCrTP
*M*1/Ti1—O1^{i}	2.065 (8) × 3	2.087 (7) × 3	2.100 (15) × 3	1.9312 (14) × 3
*M*1/Ti1—O2	2.109 (9) × 3	2.085 (8) × 3	2.097 (16) × 3	1.9559 (15) × 3
*M*2/Ti2—O3^{ii}	2.026 (7) × 3	2.014 (7) × 3	2.047 (14) × 3	1.9622 (14) × 3
*M*2/Ti2—O4	2.043 (9) × 3	2.030 (8) × 3	2.066 (18) × 3	1.9528 (15) × 3
P—O1	1.510 (8)	1.513 (8)	1.501 (16)	1.5307 (14)
P—O2	1.494 (10)	1.515 (9)	1.505 (17)	1.5338 (15)
P—O3	1.521 (7)	1.528 (7)	1.520 (14)	1.5304 (14)
P—O4	1.527 (9)	1.514 (9)	1.497 (19)	1.5244 (16)
K1—O2	3.224 (9) × 3	3.240 (9) × 3	3.246 (17) × 3	3.1108 (17) × 3
K1—O3^{ii}	2.909 (8) × 3	2.902 (7) × 3	2.921 (14) × 3	2.8220 (15) × 3
K1—O4	3.141 (9) × 3	3.199 (9) × 3	3.15 (2) × 3	3.0126 (16) × 3
K2—O1	2.907 (8) × 3	2.882 (7) × 3	2.886 (17) × 3	2.8588 (16) × 3
K2—O2^{iii}	3.145 (11) × 3	3.112 (9) × 3	3.146 (19) × 3	2.9834 (16) × 3
K2—O4$^{iii/iv}$	3.033 (9) × 3	3.023 (9) × 3	3.054 (19) × 3	2.9128 (15) × 3

Symmetry codes [KErTP and KYbTP]: (i) $-x, \frac{1}{2}+y, \frac{1}{2}-z$; (ii) $\frac{1}{2}-x, 1-y, -\frac{1}{2}+z$; (iii) $-x, -\frac{1}{2}+y, \frac{1}{2}-z$. Symmetry codes [KYTP]: (i) $-\frac{1}{2}+x, \frac{3}{2}-y, 1-z$; (ii) $\frac{1}{2}-x, 1-y, \frac{1}{2}+z$; (iii) $\frac{1}{2}+x, \frac{3}{2}-y, 1-z$. Symmetry codes [KCrTP]: (i) $-x, \frac{1}{2}+y, \frac{1}{2}-z$; (ii) $\frac{1}{2}-x, 1-y, -\frac{1}{2}+z$; (iv) $-x, -\frac{1}{2}+y, \frac{1}{2}-z$.

Table 3
Bond lengths (Å) for $KTi_2(PO_4)_3$ (Masse *et al.*, 1972) and $K_2Ti_2(PO_4)_3$ (Leclaire *et al.*, 1989).

	$KTi_2(PO_4)_3$	$K_2Ti_2(PO_4)_3$
Ti1—O1	1.925 (10) × 3	1.933 (4) × 3
Ti1—O2	1.918 (10) × 3	1.955 (4) × 3
Ti2—O3	1.965 (10) × 3	2.004 (4) × 3
Ti2—O4	1.877 (10) × 3	2.027 (4) × 3
P—O1	1.534 (11)	1.532 (4)
P—O2	1.540 (11)	1.522 (4)
P—O3	1.534 (11)	1.521 (4)
P—O4	1.536 (11)	1.539 (4)
K1—O2	3.027 (12) × 3	2.932 (4) × 3
K1—O3	2.946 (12) × 3	2.813 (4) × 3
K1—O4	3.082 (11) × 3	3.188 (4) × 3
K2—O1	2.821 (25) × 3	2.903 (4) × 3
K2—O2	2.926 (25) × 3	2.924 (4) × 3
K2—O4	2.972 (25) × 3	2.939 (4) × 3

independent octahedra in each structure. The $M1O_6$ octahedron is slightly enlarged in all rare-earth-containing langbeinites, as it is the preferred site for rare-earth atoms. The opposite is true for the chromium-containing langbeinite, and the *M* population at the preferred site is roughly two-thirds of the total site population (see supplementary material for exact numbers).

All of the new synthetic langbeinites with a rare-earth metal and titanium mixed at the same atomic sites have enlarged thermal-displacement parameters, especially for the O atoms. The thermal-displacement parameters of the O atoms for KErTP, KYbTP and KYTP are about five times as large as those of the O atoms in KCrTP (see supplementary material). This has to be attributed to the larger ionic radii of the rare-earth metals compared with that of titanium: the sum of the effective ionic radii of Ti^{IV} and O is 2.01 Å while that of M^{III} and O (M^{III} = Er, Yb or Y) is approximately 2.29 Å. In reality, the O atoms are randomly disordered at multiple sites centred at the determined atomic position. This is in order to elongate the bond distance between the rare-earth metals and neighbouring O atoms. The Ti atoms inside the octahedra are possibly at the upper limit of the bond distance between Ti and O. As expected, the thermal-displacement parameters for the O atoms in KYbTP are somewhat smaller than for KErTP and KYTP, since the effective ionic radius of ytterbium is slightly smaller than that of the other two rare-earth metals.

The volume of the M/TiO_6 octahedra is at the upper limit in terms of accommodating the Ti atoms. This is confirmed by the fact that neither praseodymium, neodymium or samarium resulted in langbeinite crystals when added to the growth flux. The cation radii of these rare-earth metals are slightly larger than those of erbium, ytterbium and yttrium (Shannon, 1976). This small increase of approximately 0.05–0.09 Å appears to eliminate the possibility of langbeinite crystallization.

The monophosphate group is regular in all $A_xMTi(PO_4)_3$ langbeinite structures (M = Ti, Cr, Er, Yb, Y), which is in agreement with the fact that the PO_4 tetrahedra are isolated from each other. The P—O bond distance varies between 1.494 (10) Å and 1.5338 (15) Å with tetrahedra angles in the range 106.0 (5)–112.0 (8)°. The P—O bond lengths are practically equal in the different compounds with the exception of a small shrinkage for the rare-earth-containing phosphate langbeinites (Tables 2 and 3). This is an effect of the enlarged atomic thermal-displacement parameters in those structures.

The two crystallographically independent cation sites are separated by 3.8205 (7) Å in KCrTP and 3.958 (2) Å in KErTP. Bond distances between the coordinating O atoms and respective cation sites vary. KCrTP has K1—O bond distances of 2.8220 (15)–3.1108 (17) Å and K2—O bond distances of 2.8588 (16)–2.9834 (16) Å, whereas KErTP has bond distances of 2.909 (8)–3.224 (9) Å and 2.907 (8)–3.145 (11) Å, respectively. Table 2 gives a complete list of K—O bond distances for KErTP, KYbTP, KYTP and KCrTP. The mean K—O bond distance in all structures is significantly shorter at the K2 site, and this trend is also present in all $K_{1+x}M_xTi_{2-x}(PO_4)_3$ structures. Table 3 gives bond distances for the $KTi_2(PO_4)_3$ and $K_2Ti_2(PO_4)_3$ structures. This results in a constrained K2 site in all non-rare-earth-containing $K_{1+x}M_xTi_{2-x}(PO_4)_3$ structures. The preferred cation site is K1

in both $K_{1.75}Ti_2(PO_4)_3$ and $KTi_2(PO_4)_3$ (Leclaire *et al.*, 1989; Masse *et al.*, 1972). The increased cell volume is due to the inclusion of a rare-earth metal in the $K_2MTi(PO_4)_3$ structures (M = Er, Yb, Y) and results in two equally good cation sites, which in turn gives a structurally determined Ti/M ratio of 1:1.

Financial support from the Swedish Research Council and the Chalmers Foundation is gratefully acknowledged. The author is indebted to Professor Jörgen Albertsson and Dr Göran Svensson for helpful discussions.

References

Abrahams, S. C. & Bernstein, J. L. (1977). *J. Chem. Phys.* **67**, 2146–2150.

Alcock, N. W. (1974). *Acta Cryst.* A**30**, 332–335.

Bolt, R. J. (1993). *J. Cryst. Growth*, **126**, 175–178.

Boudjada, A. & Perret, R. (1977). *J. Appl. Cryst.* **10**, 129.

Brezina, B. & Glogarova, M. (1972). *Phys. Status Solidi A*, **11**, K39–K42.

Cord, P. P., Courtine, P. & Pannetier, G. (1971). *Bull. Soc. Chim. Fr.* **7**, 2461–2465.

Enraf–Nonius (1989). *CAD-4 Software*. Version 5.0. Enraf–Nonius, Delft, The Netherlands.

Flack, H. D. (1983). *Acta Cryst.* A**39**, 876–881.

Genkina, E. A., Kalinin, V. B., Maksimov, B. A. & Golubev, A. M. (1991). *Sov. Phys. Crystallogr.* **36**, 636–639.

Guelylah, A., Madariaga, G., Morgenroth, W., Aroyo, M. I., Breczewski, T. & Bocanegra, E. H. (2000). *Acta Cryst.* B**56**, 921–935.

Hall, S. R., du Boulay, D. J. & Olthof-Hazekamp, R. (2000). Editors. *Xtal*3.71, *System of Crystallographic Programs.* University of Western Australia, Australia.

Hamilton, W. C. (1964). *Statistics in Physical Science.* New York: Ronald Press.

Hazen, R. M., Palmer, D. C., Finger, L. W., Stucky, G. D., Harrison, W. T. A. & Gier, T. E. (1994). *J. Phys. Condens. Matter*, **6**, 1333–1344.

Hikita, T., Kudo, T., Chubachi, Y. & Ikeda, T. (1976). *J. Phys. Soc. Jpn*, **41**, 349–350.

Isasi, J. & Daidouh, A. (2000). *Solid State Ion.* **133**, 303–313.

Ivanov, Y. A., Belokoneva, E. L., Egerov-Tismenko, Y. K., Simonov, M. A. & Belov, N. V. (1980). *Sov. Phys. Dokl.* **252**, 420–422.

Jacco, J. C., Loiacono, G. M., Jaso, M., Mizell, G. & Greenberg, B. (1984). *J. Cryst. Growth*, **70**, 484–488.

Jona, F. & Pepinsky, R. (1956). *Phys. Rev.* **103**, 1126–1130.

Klevtsov, P. V., Kim, V. G., Kletsova, R. F., Glinskaya, L. A. & Solodovnikov, S. F. (1988). *Sov. Phys. Crystallogr.* **33**, 30–33.

Kohler, K. & Franke, W. (1964). *Acta Cryst.* **17**, 1088–1089.

Larson, A. C. (1970). *Crystallographic Computing*, edited by F. R. Ahmed, S. R. Hall & C. P. Huber, pp. 291–294. Copenhagen: Munksgaard.

Leclaire, A., Benmoussa, A., Borel, M. M., Grandin, A. & Raveau, B. (1989). *J. Solid State Chem.* **78**, 227–231.

Lissalde, F., Abrahams, S. C., Bernstein, J. L. & Nassau, K. (1979). *J. Appl. Phys.* **50**, 845–851.

Lunezheva, E. S., Maksimov, B. A. & Mel'nikov, O. K. (1989). *Sov. Phys. Crystallogr.* **34**, 674–676.

Masse, R., Durif, A., Guitel, J. C. & Tordjman, I. (1972). *Bull. Soc. Fr. Mineral. Cristallogr.* **95**, 47–55.

Moriyoshi, C., Itoh, K. & Hikita, T. (1996). *Physica B*, **219/220**, 602–604.

Norberg, S. T., Streltsov, V. A., Svensson, G. & Albertsson, J. (2000). *Acta Cryst.* B**56**, 980–987.

Percival, M. J. L., Schmahl, W. W. & Salje, E. (1989). *Phys. Chem. Min.* **16**, 569–575.

Perret, R. (1988). *J. Less-Common Met.* **144**, 195–200.

Perret, R. & Boudjada, A. (1979). *C. R. Acad. Sci. Ser. C*, **288**, 525–527.

Rangan, K. K. & Gopalakrishnan, J. (1994). *J. Solid State Chem.* **109**, 116–121.

Shannon, R. D. (1976). *Acta Cryst.* A**32**, 751–767.

Sheldrick, G. M. (1997). *SHELXS*97. *Program for Solving of Crystal Structures.* University of Göttingen, Germany.

Sljukic, M., Matkovic, B., Prodic, B. & Scavnicar, S. (1967). *Croat. Chem. Acta*, **39**, 145–148.

Slobodyanik, N. S., Stus, N. V., Nagornyi, P. G. & Kapshuk, A. A. (1991). *Rus. J. Inor. Chem.* **36**, 1554–1556.

Tordjman, I., Masse, R. & Guitel, J. C. (1974). *Z. Kristallogr.* **139**, 103–115.

Von Alpen, U., Bell, M. F. & Wichelhaus, W. (1979). *Mater. Res. Bull.* **14**, 1317–1322.

Yamada, N., Maeda, M. & Adachi, H. (1981). *J. Phys. Soc. Jpn*, **50**, 907–913.

Zachariasen, W. H. (1967). *Acta Cryst.* **23**, 558–564.

Zemann, A. & Zemann, J. (1957). *Acta Cryst.* **10**, 409–413.